Polymer 51 (2010) 709–718

Contents lists available at ScienceDirect

Polymer

journal homepage: www.elsevier.com/locate/polymer

Polyurethane–POSS hybrids: Molecular dynamics studies

K.N. Raftopoulos [a], Ch. Pandis [a], L. Apekis [a], P. Pissis [a,*], B. Janowski [b], K. Pielichowski [b], J. Jaczewska [c,d]

[a] Department of Physics, National Technical University of Athens, Iroon Polytechneiou 9, Zografou, Campus, 157 80, Athens, Greece
[b] Department of Chemistry and Technology of Polymers, Krakow University of Technology, ul. Warszawska 24, 31-155 Krakow, Poland
[c] M. Smoluchowski Institute of Physics, Jagiellonian University, ul. Reymonta 4, 30-059 Krakow, Poland
[d] The Henryk Niewodniczanski Institute of Nuclear Physics, Polish Academy of Sciences, ul.Radzikowskiego 152, 31-342 Krakow, Poland

ARTICLE INFO

Article history:
Received 22 June 2009
Received in revised form
5 November 2009
Accepted 23 November 2009
Available online 4 December 2009

Keywords:
Dielectric spectroscopy
Polyurethane–POSS nanocomposites
Polymer dynamics

ABSTRACT

A series of hybrid polyurethane–POSS materials have been synthesized on the basis of poly(tetramethylene glycol) (Terathane 1400®) as soft component, 4,4′-methylenebis(phenylisocyanate) (MDI) as hard component, and 1,4-butanediol as chain extender. POSS particles properly modified have been tethered on the main chain by substitution of the chain extender to weight fractions up to 10%. AFM measurements indicate the formation of POSS crystallites in the PU matrix, extended structures at low POSS content and more regular, smaller structures at higher POSS content. A detailed investigation of molecular mobility by means of Differential Scanning Calorimetry (DSC), Thermally Stimulated Depolarization Currents (TSDC) and, mainly, Broadband Dielectric Relaxation Spectroscopy (DRS) has been conducted in all samples of the series and in addition in neat Terathane, as reference. Four relaxations have been studied in detail: two secondary relaxations γ and β, the segmental α relaxation (dynamic glass transition) and an α' relaxation slower than α associated with crystallinity in neat Terathane and with the presence of hard microdomains in the polyurethane and the hybrids. Secondary relaxations remain unaffected by POSS. The glass transition temperature rises by a few degrees and, in consistency with that, segmental dynamics slightly slows down with increasing POSS content. In addition, the dielectric strength of the segmental relaxation decreases with increasing POSS content, suggesting that a fraction of polymer is immobilized, making no contribution to the relaxation. These results are discussed in relation to morphology.

1. Introduction

Advances in technological applications demand for the development of materials with tailor-made properties well tuned to modern needs. One component materials or even two phase materials are not sufficient to meet those demands. Therefore, research has been directed to composite materials with fillers with typical dimensions in the order of magnitude of nanometer (nanocomposites) or materials forming structures in the same order of magnitude (nanostructured materials) [1]. Polymeric materials proved to be ideal matrices for those families of materials due to their ease of synthesis and processability, as well as the versatile chemical structures that carbon and different heteroatoms are able to form.

Properties of the aforementioned nanocomposites depend not only on the matrix and filler physical and chemical properties but also on their mutual interactions which become prominent due to the enormous interfacial area over material volume ratio. Fillers may be incorporated in the matrix either by mixing (i.e. in the resulting materials, filler is not tied by chemical bond to the polymeric chain), grafting (fillers are chemically bonded to the chains?) or employed in polymerization as building blocks (nanobuilding blocks) [2]. The later approach allows for better control on the arrangement of the particles in the nanoscale dimension [3–5].

Segmented polyurethanes (PUs) are linear block copolymers of the-$[A–B]_n$-type. They consist of the relatively flexible (rubbery) soft segments (SS) and the relatively rigid (solid like) hard segments (HS). SS are normally formed of a flexible macrodiol while HS are formed by the reaction of a rigid diisocyanate with either diol or diamine molecules which act as chain extenders. The two components are thermodynamically incompatible to each other, thus forming a material with morphology consisting of microdomains rich in HS and a microphase rich in SS. This so-called microphase separation is responsible for the exceptional properties of this kind of materials [6,7]. The glassy or semicrystaline HS domains act as physical crosslinks and reinforcing fillers, while SS domains provide the characteristic flexibility of PUs [8]. Several factors affect the degree of microphase separation including

* Corresponding author. Tel.: +30 210 7722986; fax: +30 210 7722932.
E-mail address: ppissis@central.ntua.gr (P. Pissis).

0032-3861/$ – see front matter © 2009 Elsevier Ltd. All rights reserved.
doi:10.1016/j.polymer.2009.11.067

polarity of the SS and HS and flexibility of HS [8]. Physical properties of PUs, like glass transition temperature (T_g), depend strongly on the degree of microphase separation [9].

On the other hand, polyhedral oligomeric silsesquioxanes (POSS) particles are cage like structures of the $(RSiO_{1.5})_n$ type. R might be H, or a variety of organic groups fixed onto the Si atoms on the corners of the cage, and is used to optimize polymer–POSS interaction and simultaneously to aid in dissolution in common solvents for synthesis purposes. Consequently, POSS particles are ideal nanobuilding blocks for synthesis of organic-inorganic hybrid materials [3–5]. Incorporation of POSS in polymers results in improvement of properties, such as mechanical properties, thermal stability [10], flammability, gas permeability and dielectric permittivity [5].

Previous research has shown that in polymer–POSS composites synthesized by physical mixing POSS–POSS interactions dominate due to crystallization and aggregation of particles, while POSS–polymer interaction becomes more important in the case POSS particles are used as nanobuilding blocks [11]. However, even in the latter case, POSS–POSS interaction may as well highly affect physical properties of the polymer matrix [12], which can be related with POSS crystallization observed by Fu et al. [13], as well as POSS aggregation and formation of multilevel structural organization observed by Bliznyuk et al. [6]. Regarding the segmental dynamics of such systems, Zhao and Schiraldi [14], have observed plasticization (reduction of glass transition temperature, T_g) in untethered polycarbonate-POSS systems. Xu et al. [15] observed in tethered systems the same phenomenon at low POSS contents, however, upon increasing the latter, the opposite behavior was observed, i.e. increase of T_g due to increased POSS–POSS and POSS–polymer interactions. Kopesky et al. [16] have compared the behavior of segmental dynamics of PMMA with tethered and untethered POSS particles and observed slowing down of dynamics in the first case while in the latter a decrease of viscosity was observed attributed to increase of free volume. Acceleration of dynamics upon addition of POSS was also observed by Kourkoutsaki et al. [17] in rubbery epoxy resin systems with POSS as dangling moieties by means of dielectric techniques, and attributed to increase of free volume; however, the magnitude (dielectric strength) of the segmental relaxation was significantly reduced on addition of POSS, indicating that a fraction of polymer was immobilized at the interfaces with POSS particles. Acceleration of the segmental α relaxation, as well as of the secondary β relaxation, was observed by dielectric spectroscopy also in polycarbonate-POSS nanocomposites prepared by solution blending and explained in terms of plasticization due to increase of free volume rationalized by density measurements [18].

It becomes clear from this short survey that, despite the increasing attention of the polymer community and numerous publications, more work is needed to further clarify and quantify the factors which affect molecular dynamics, in particular segmental dynamics and glass transition, in polymer-POSS nanocomposites. In addition to fundamental interest, the investigation of polymer dynamics forms an essential part of the investigation of structure–property relationships in polymer nanocomposites. A true understanding of these relationships is a prerequisite for optimizing composition and preparation/processing conditions and preparing materials with predicted properties tailored to end-use requirements [5,17]. The task becomes more complicated if intrinsically complex systems, like segmented PUs in this work, are used as polymer matrix. Previous work in PU-POSS composites using POSS particles as nanobuilding blocks indicated POSS aggregation and formation of multilevel structural organization [6]. The glass transition temperature was found to increase on incorporation of POSS in PU networks due to increase of cross-linking density and the reinforcement effect of the POSS cages [10,19].

The present work deals with molecular dynamics studies in nanocomposites prepared by incorporating modified POSS particles in the main chain of a typical segmented PU, by using differential scanning calorimetry (DSC) and two dielectric techniques, broadband dielectric relaxation spectroscopy (DRS) and thermally stimulated depolarization currents (TSDC). Special attention was paid to quantification of the effects of nanoparticles on molecular dynamics of the polymer matrix in terms of fraction of polymer modified and type and degree of modification. Combination of the three techniques, DSC/DRS/TSDC, in previous work on other polymer nanocomposites has proved very effective in that respect [17,20,21]. In the present work, the results obtained by the three techniques together lead to the conclusion that a fraction of the PU matrix is immobilized making no contribution to the glass transition and the rest shows moderate slowing down of segmental dynamics (increase of T_g). Proper analysis of the experimental data enables quantification of these results. In addition to "direct" effects of nanoparticles in the case of a homogeneous polymer matrix, "indirect" effects may be expected when the polymer matrix is microphase-separated, like in PUs, arising from a possible modification of the degree of microphase separation in the nanocomposites. The TSDC results for the interfacial polarization/relaxation characteristic for the microphase separation of the PU matrix show that the microphase-separated structure of the PU matrix is not modified on addition of POSS, providing evidence that the effects on polymer dynamics observed are "direct" reinforcement effects. Morphology of the nanocomposites was investigated by atomic force microscopy (AFM) and a correlation was observed between the size of crystalline POSS structures and the extent of slowing down of segmental dynamics in the nanocomposites. Previous work on the same materials using thermogravimetric analysis indicated an increase in thermal stability on addition of POSS [22]. The results obtained within the present study provide a reasonable explanation of the improved thermal stability of the nanocomposites in terms of restricted segmental dynamics.

Preliminary results of the present work have been published in the proceedings of the 3rd International Seminar on Modern Polymeric Materials for Environmental Applications [23].

2. Experimental

2.1. Materials

The polyurethane matrix was prepared by reaction of 4,4′-methylenebis(phenylisocyanate) (MDI) as isocyanate component and poly(tetramethylene glycol) (Terathane 1400®) (Invista) with molecular weight of ~1400 as elastic component. 1,4-butanediol (Aldrich) was used as chain extender. Nanocomposites were prepared by appropriate substitution of chain extender by 1,2-propanediol-heptaisobutyl-POSS (PHIPOSS) (Hybrid Plastics) in order to provide samples with POSS mass fractions of 2–10%. Mass fraction of elastic component in the polyurethane is 50%. For comparison, pure Terathane 1400 was also studied.

2.2. Preparation of polyurethane/POSS nanohybrid elastomers

MDI was charged into a 100 ml three-necked round bottomed flask, equipped with a mechanical stirrer and nitrogen inlet. It was melted at 70 °C and PHIPOSS solution in suitable amount of Terathane was then added in one portion. Previously the PHIPOSS mixture in Terathane was heated to 120 °C to dissolve the POSS

cages in the polyol and then cooled to 60 °C. The reaction was performed under a nitrogen atmosphere at 80 °C for 2 h to form a polyurethane prepolymer. The NCO groups content was then determined and the prepolymer was mixed with suitable amount of 1,4-butanediol. The mixture was poured out on Petri dish and cured at 110 °C for 2 h and post-cured at 80 °C for 16 h.

In the following samples will be denoted as PUXX with XX being the wt% fraction of POSS in the final material. Terathane will be denoted as T1400.

2.3. Morphology–Atomic force microscopy (AFM)

AFM studies were performed for two selected compositions. The AFM images were recorded by means of an XE 120 atomic force microscope (Park Systems, Korea) in contact mode, using Si3N4 tips (VEECO, USA) with spring constant of 0.03 N/m.

2.4. Differential scanning calorimetry (DSC)

Differential Scanning Calorimetry thermograms were recorded on a Pyris 6 heat flux Differential Scanning Calorimeter (Perkin Elmer, USA) in the temperature range −120 to +45 °C, with specimens of mass ~10 mg placed in standard aluminum pans provided by the same company. Heating-cooling rate was 10 deg/min. Second runs (to delete thermal history) were used for evaluation.

2.5. Thermally stimulated depolarization currents (TSDC)

Thermally Stimulated Depolarization Currents (TSDC) is a special dielectric technique in the temperature domain, which corresponds to measuring dielectric losses as a function of temperature at fixed low frequencies in the range (10^{-4}–10^{-2} Hz) [24]. The technique is characterized by high sensitivity and, owing to its low equivalent frequency, by high resolving power [24,25].

By this technique the sample is placed between the plates of a capacitor and heated to a temperature T_p, where a dc field of the order of 1 MV/m is applied to the capacitor for time t_p, which is by orders of magnitude higher than the relaxation time of the mechanism under investigation at this temperature. Subsequently, with the field still applied, the sample is cooled down to a temperature T_d at which the relaxation time of the mechanism under investigation becomes orders of magnitude higher than the time of the experiment. The dc field is switched off, the capacitor is connected to a sensitive electrometer and the sample is heated at a constant rate b while the depolarization current is recorded.

In our study, a Keithley 617 programmable electrometer was used to measure the current and control voltage in combination with a home-made amplifier. Temperature control was achieved by means of a Quatro cryosystem (Novocontrol, Germany). The sample (of square shape, surface area 20 × 20 mm, thickness 1–2 mm) was placed in a Novocontrol TSDC sample cell. Measurement parameters for all samples were $T_p = 25$ °C, $t_p = 5$ min, $T_d = -150$ °C and $b = 3$ deg/min.

2.6. Dielectric relaxation spectroscopy (DRS)

Specimens for DRS measurements were the same as those used for TSDC. Measurements were performed with an Alpha Analyzer combined with a Quatro Temperature Control system, both by Novocontrol. Complex dielectric permittivity $\varepsilon^*(f) = \varepsilon'(f) - i\varepsilon''(f)$ was measured isothermally in steps of 5 °C in the temperature interval −150 to +45 °C and in the frequency range from 10^{-1} (10^{-2} in specific cases to follow slow processes) to 10^6 Hz. Detailed description of the method may be found in [26].

3. Results and discussion

3.1. Morphology

Wide-angle X-ray diffraction (WAXD) measurements to be reported in detail elsewhere showed that the neat PU is amorphous, and the same is true also for the PU matrix in the hybrids. Sharp maxima of small intensity in the hybrids at about 8° indicated POSS molecules aggregation and crystallization, which was further studied here by AFM. Fig. 1 shows lateral force AFM images for samples PU04 and PU10 at various magnifications. For the sample with the smaller filler content, the POSS molecules aggregate to nanometer size longitudinal crystallites (about 60–70 nm in length) (Fig. 1, top), which form spherulites of several microns average sizes (Fig. 1, bottom left). At higher filler content (PU10), POSS forms more regular crystallites of about 120 nm sizes (Fig. 1, bottom right). These observations indicate that PHIPOSS shows strong tendency to form crystallites in PU matrix, however of different types, i.e. extended structures for PU04 and more regular, smaller structures for the higher POSS content (PU10). An interesting question in the following will be as to whether and how this different morphology is reflected in polymer dynamics.

3.2. Differential scanning calorimetry

The DSC thermograms obtained with the PU matrix and the hybrids are shown in Fig. 2. A step corresponding to glass transition is visible in the temperature range −70 to −40 °C. Glass transition temperatures (T_g) obtained as the maximum of the derivative of heat flow are also plotted against POSS fraction in Fig. 3 (together with other measures of glass transition temperature to be reported in the next sections). It should be mentioned that, in consistency with the results of WAXD measurements in Section 3.1, no indication of melting or crystallization is observed in the temperature range of the measurements, providing additional evidence for the amorphous character of the PU matrix and the hybrids.

In the DSC thermogram for pure Terathane (figure in electronic supplementary material) a strong endothermic peak at 26 °C is dominant and is attributed to melting of the crystallization (in agreement with information provided by the supplier). A weak step in heat capacity at ~ −80 °C is attributed to the glass transition of the amorphous Terathane phase.

T_g of the neat PU matrix is higher by ~25 °C than that of pure Terathane, indicating radical reduction of mobility of Terathane chains in PU. It is well established that this reduction of molecular mobility arises from the presence of and interaction with the hard microdomains and the incomplete microphase separation [9]. In the hybrids, T_g increases moderately but systematically upon addition of POSS particles (Fig. 3). More specifically, a moderate increase of T_g is observed in the region of 2–4%, followed by a plateau up to 4–6% and a more prominent increase at higher POSS contents.

So far, experimental data confirm results by Kopesky [16] in tethered systems. Reduction of T_g at low POSS contents observed by Xu [15] is not observed; however, the plateau observed in Fig. 3 indicates the existence of a factor that tends to increase mobility, presumably increase of free volume. Thus, we may attribute the behavior observed in Fig. 3 to two contradictory effects, i.e. increase of free volume due to loosened molecular packing of the chains, on the one hand, and constraints imposed by physical cross-linking, implying more rigid structure of the chain, on the other hand [27]. The steep increase of T_g at higher POSS contents may be correlated with the results of AFM measurements reported above, which show that the crystals formed in PU10 are smaller, of the order of magnitude of nm, as compared to PU04. As a result, the POSS

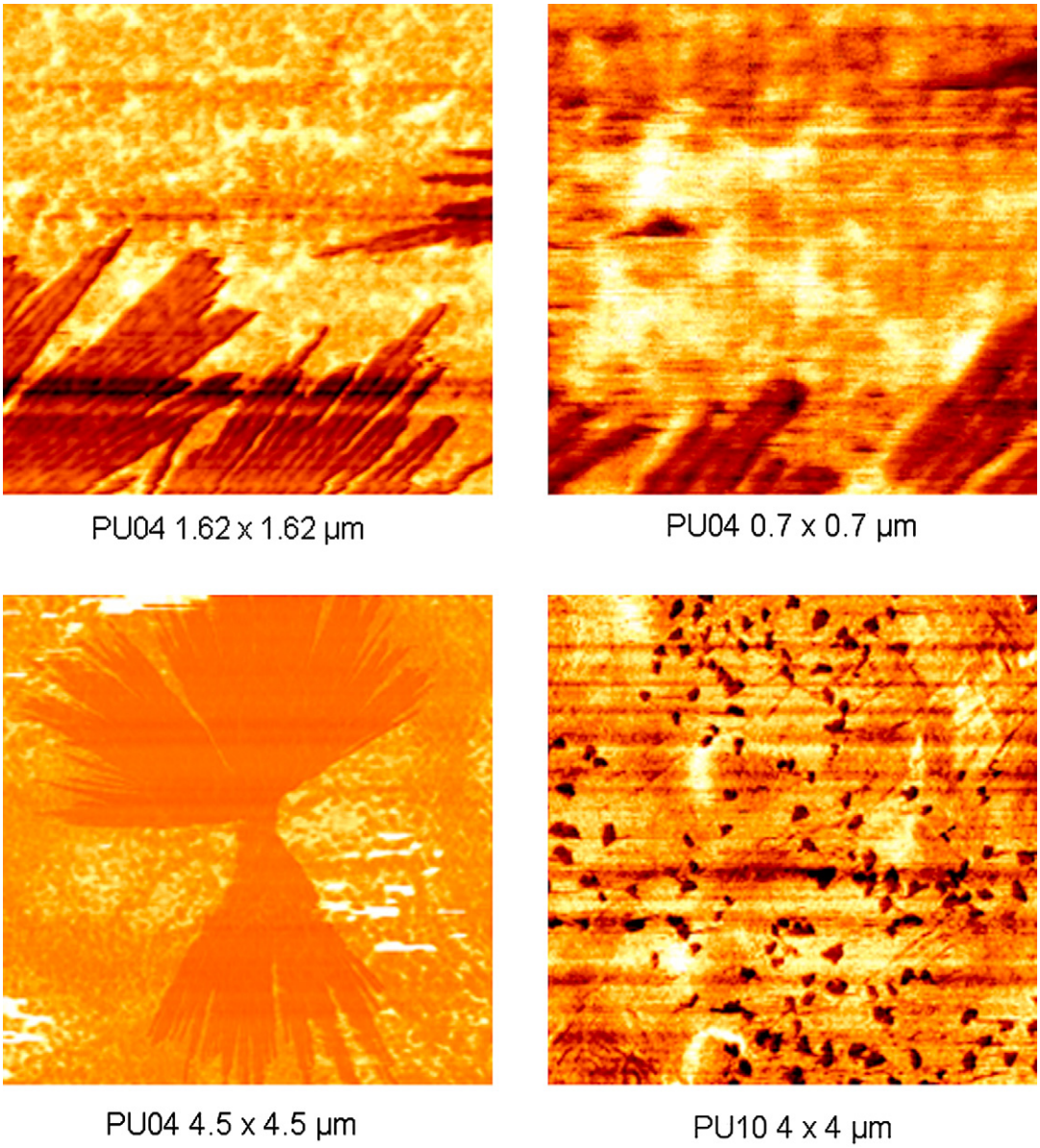

Fig. 1. Lateral force AFM images for PU04 (area1.62 × 1.62 μm, top left; 0.7 × 0.7 μm, top right; 4.5 × 4.5 μm, bottom left) and for PU10 (4 × 4 μm, bottom right).

crystals exhibit higher surface-to-volume ratio in PU10, thus their effect is expected to be more prominent. Further confirmation of the dependence of T_g on POSS content is provided by the two dielectric techniques employed in this study and will be discussed later in this paper.

3.3. Thermally stimulated depolarization currents (TSDC)

TSDC thermograms recorded with all materials under investigation were normalized to the same electrode area and polarization field by, $I_n = (I \cdot d)/(A \cdot V)$, where I is the measured current, d is the sample thickness, A the electrode area and V the applied voltage. Different samples can then be directly compared to each other with respect to the magnitude (intensity) of a peak, i.e. the relaxation strength of the corresponding relaxation [24]. Normalized thermocurrents are shown in Fig. 4. For the neat PU matrix and the hybrids, 3 relaxations can be observed. Starting from low temperatures, the β relaxation is visible as a rather broad peak at about −120 °C, attributed by the literature [28] to the movements of polar carbonyl groups with attached water molecules. In the region of −60 °C a stronger peak is observed, which corresponds to the α relaxation associated with the glass transition. Owing to the approximately similar time scales of DSC and TSDC, the peak temperature (temperature of current maximum) of that peak is a good measure of calorimetric T_g [29]. Finally, in the region 0–10 °C, a more prominent peak is observed, which is attributed to the interfacial Maxwell–Wagner–Sillars (MWS) polarization and relaxation due to accumulation of charges at the interfaces of regions (microphases) with different conductivity, namely the hard microdomains and the soft microphase of PU [30,31].

For T1400 one can observe in Fig. 4, in the order of increasing temperature, the β relaxation as a weak shoulder on the low temperature side of the α relaxation, which is located at about −80 °C. A prominent peak following the α relaxation at about −20 °C may be associated with interfacial polarization (MWS), now at the interfaces between crystalline and amorphous parts of the polymer.

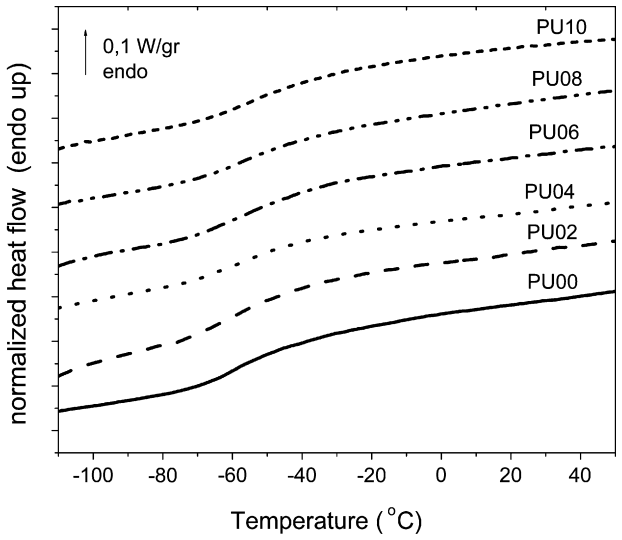

Fig. 2. Normalized DSC thermograms (second run) recorded with polyurethane matrix and the hybrids at a rate of 10 deg/min. For clarity, curves have been shifted vertically.

In consistency with that interpretation, the MWS peak is at a lower temperature than the melting peak observed by DSC at 26 °C.

The β relaxation seems to be unaffected by the addition of POSS. This should be expected due to its local character [32], and has been recently reported also for PU/clay nanocomposites [21].

The peak temperature of the α relaxation (T_α) follows the same trends with the calorimetric T_g, being always (with the exception of PU06) about 2 °C lower than the latter (Fig. 3). This small difference may be attributed to fine differences in the equivalent frequencies (time scales) of the two methods and/or possible differences in the type of motions probed by the two techniques at the glass transition [29]. The strength of the relaxation, as quantified by the magnitude (intensity) of the peak, is reduced overproportionally to the reduction of the Terathane mass fraction in the final material (please note the logarithmic scale in Fig. 4). We interpret this result in terms of a fraction of polymer making no contribution to the α relaxation (dynamic glass transition), i.e. being immobilized, probably at interfaces with the POSS molecules/crystallites [20,33]. Similar results were obtained in previous work with poly(dimethyl siloxane)/silica [20], rubbery epoxy networks/POSS [17] and

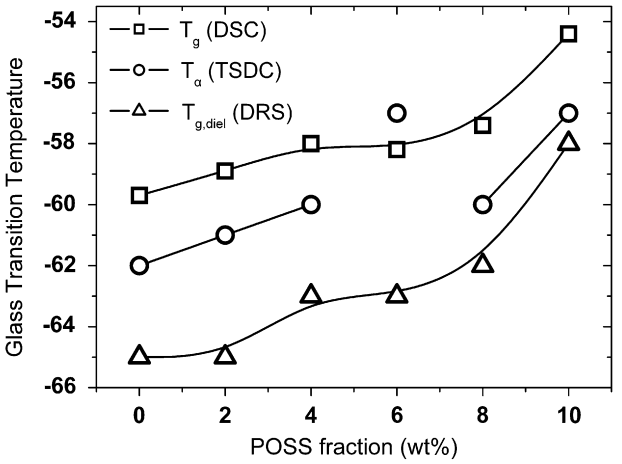

Fig. 3. Glass transition temperatures as observed by the three techniques indicated on the plot against POSS content. Lines are guides to the eye.

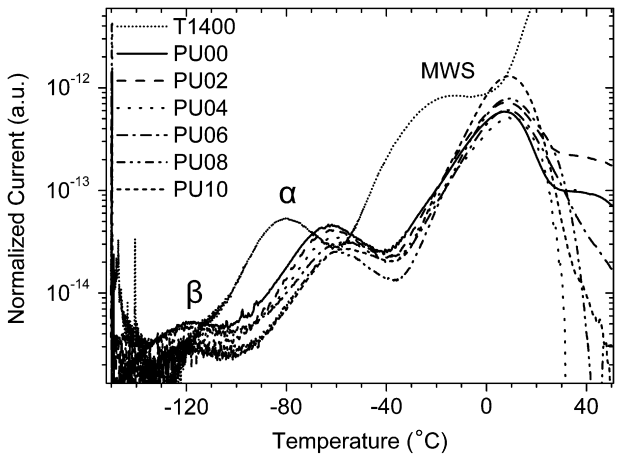

Fig. 4. Normalized TSDC thermograms for all materials under investigation.

PU/clay [21] nanocomposites. In order to quantify this result, first the maximum depolarization current I_m was normalized to the same polymer fraction by $I_{m,n} = I_m/(1 - w)$, where w is the weight fraction of POSS in the hybrids; then the fraction of immobilized polymer χ_{im}, was calculated by $\chi_{im}=(I_{m0} - I_{m,n})/I_{m0}$, where I_{m0} is the maximum depolarization current in neat PU. Please note that for a more accurate calculation the dielectric strength $\Delta\varepsilon$, obtained from the surface area under the TSDC α peak [24], rather than I_m, should be in general considered [17,20]. That was, however, not possible in the present work, because of the background in Fig. 4 increasing with increasing temperature. Fig. 5 shows values of χ_{im}, calculated by the procedure described above and by three more methods based on DRS results to be described in the next section, as a function of POSS content in the hybrids. We will comment on these results later in the next section.

A final comment in this section refers to the MWS interfacial relaxation in relation to polymer dynamics in the hybrids. No significant effects of POSS on the characteristics of the MWS peak, in particular its temperature position, are observed in Fig. 4, indicating, on the basis of previous work by TSDC in PUs [25,30,34], that the microphase-separated morphology of the PU matrix is not significantly altered on addition of POSS. Thus, the increase of T_α (and of T_g) with increasing POSS content in Fig. 3 does not arise from any changes in microphase separation of the PU matrix [9,30], but rather from constraints imposed to the motion of the PU chains

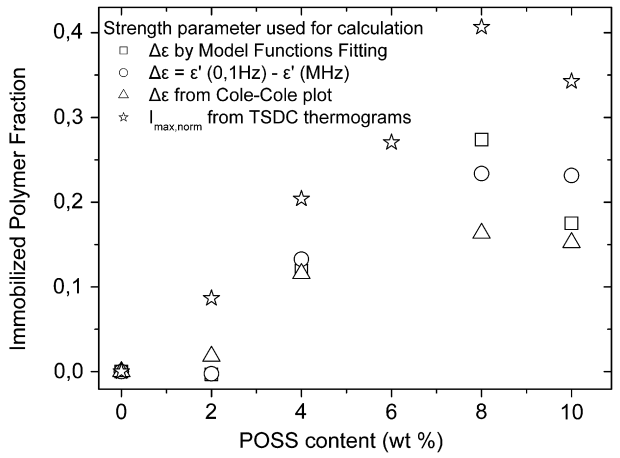

Fig. 5. Immobilized polymer fraction χ_{im} determined by various methods indicated on the plot against POSS content of the hybrids.

by the POSS molecules/crystallites, as discussed above. This is a significant result with respect to both morphology in the hybrids (the addition of POSS molecules does not alter significantly the degree of microphase separation of the PU matrix) and dynamics (the effects of POSS molecules on polymer dynamics observed, immobilization and slowing down of segmental dynamics, are "direct" reinforcement effects).

3.4. Dielectric relaxation spectroscopy (DRS)

Typical dielectric loss (ε'') spectra recorded with a selected sample for various temperatures are shown in Fig. 6. Four relaxations are observed. The γ relaxation is visible in a wide temperature interval, followed by the weak β relaxation which is visible only in a short temperature interval (-70 to -55 °C) before being masked by the α relaxation. Between the α peak and the combined contribution of dc conductivity and MWS (steep increase of $\varepsilon''(f)$ with decreasing frequency in the low frequency region) a weak relaxation, which will be designated as α' in the following, is present as a shoulder, as confirmed by the fitting in Fig. 6 (to be discussed later in the section "Analysis"). Plasticization of the α relaxation (acceleration of dynamics) in hydrated samples, which will be discussed briefly later in this work, revealed more clearly the presence of the α' relaxation.

4. Qualitative observations

Before we proceed with analysis of the DRS data, similar to those shown in Fig. 6, we try to extract as much information as possible from the raw data. In order to provide a more comprehensive overview of the aforementioned relaxations (and enable direct comparison with the TSDC thermograms in Fig. 4), ε'' data at a fixed frequency of 20 Hz taken from the isothermal spectra have been replotted as a function of temperature and are shown for all samples in Fig. 7. In this plot γ is clearly observed at -125 °C for all materials. The β relaxation of neat polyurethane and the hybrids is observed as a weak shoulder at the low-temperatures side of α, but for T1400 it is completely masked by the latter. The α peak is observed at -70 °C for Terathane while for the polyurethane and the hybrids it lies in the region -50 to -30 °C with systematic variation of its peak temperature similar to that observed for the TSDC α peak in Section 3.3 and the calorimetric T_g in Section 3.2. For

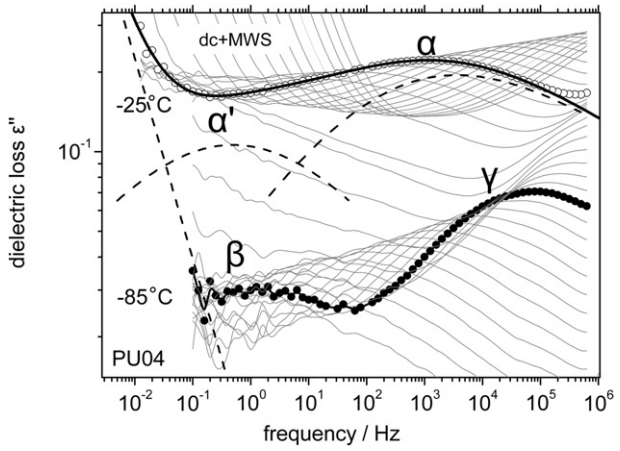

Fig. 6. Dielectric loss spectra recorded with PU04 in the temperature range -150 to $+45$ °C in step of 5 °C. Spectra at temperatures where relaxations are well observed are plotted as circles for clarity. Dashed lines represent three components of the complex spectrum at 25 °C determined by the fitting procedure described in detail in text. Thick continuous line is their sum.

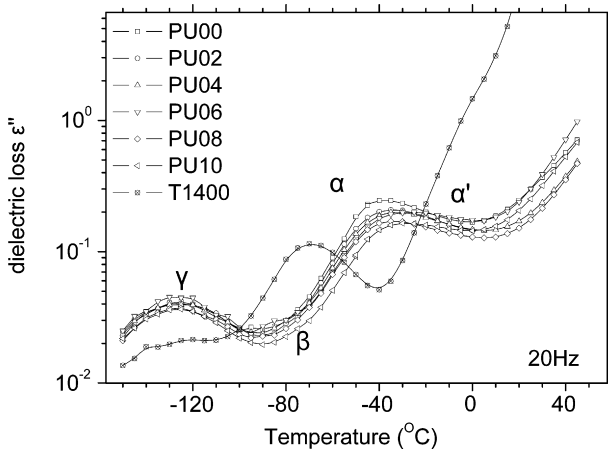

Fig. 7. Comparative isochronal plots for all materials under investigation at a frequency of 20 Hz.

the polyurethane and the composites, α' can only be distinguished as an unusually moderate slope between the α peak and the combined contribution of MWS and dc conductivity, that follows. For Terathane, in the same temperature as α' of the matrices, a shoulder on the dc effect can be observed.

Fig. 8 shows comparative dielectric spectra for the neat polyurethane matrix and the hybrids at -25 °C to follow the α and α' relaxations. In a similar plot at -85 °C, in electronic supplementary material, no variation of the time scale (frequency position) of the two local γ and β relaxations is observed upon modification by PHIPOSS, in agreement with the TSDC data in Fig. 4 and the isochronal DRS data in Fig. 7. The maximum dielectric loss (magnitude) of the two secondary relaxations decreases slightly in the hybrids, although not systematically with composition. The decrease may be well attributed to the reduction of Terathane mass fraction in the hybrid materials due to addition of PHIPOSS, whereas the unsystematic variation with composition may be explained by the inaccuracy in the determination of the thickness of the samples. The α relaxation, as observed at -25 °C (Fig. 8), becomes slower with increasing POSS content, indicating reduced mobility in the hybrids. This result is in agreement with the DSC and the TSDC results reported in previous sections that show increase of T_g upon addition of POSS. This behavior, properly

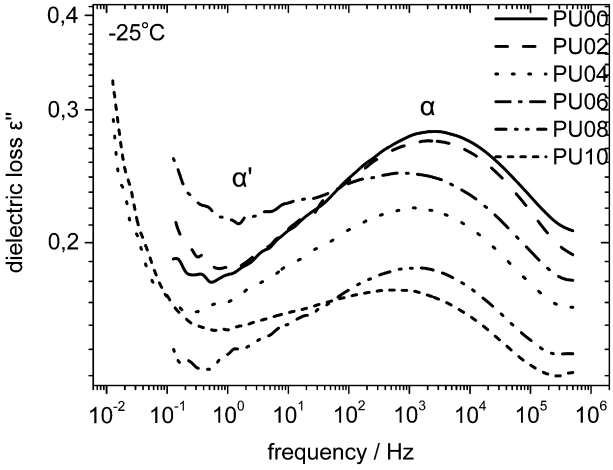

Fig. 8. Comparative dielectric loss spectra of the polyurethane matrix and the composites at -25 °C.

quantified, will be further discussed later after analysis. The magnitude of the relaxation decreases significantly in the hybrids. Similar to the TSDC results, this decrease is more intense than expected due to reduced mass fraction of polyurethane chains and may be due to immobilized polymer fraction as discussed in Section 3.3 (Fig. 5). We will come back to this point later after proper analysis of the DRS data.

4.1. Effects of water

In order to further clarify the existence of the two, not well resolved by DRS relaxations, i.e. β and α', measurements at different hydration levels have been performed for three selected samples (PU00, PU04 and PU08). Previous work on polyurethane samples at different hydration levels has indicated significant effects of water on the β and α relaxations [35]. Samples were left to equilibrate inside desiccators with i) water absorbing agent (P_2O_5, dry sample) and ii) saturated aqueous solution of KNO_3 (relative humidity 95%, hydrated sample) and then measured according to the aforementioned protocol. Results for the pure matrix for two selected temperatures are shown in Fig. 9. The local γ relaxation is not affected at all by the presence of water, while β is clearly enhanced, although without any observable influence on its time scale, indicating that water acts as probe for the type of dipole associated with this relaxation, without affecting their actual mobility. The segmental dynamics is clearly accelerated (plasticization effect). Due to plasticization, the α' relaxation is resolved from the α relaxation and for the hydrated sample it is clearly seen as a shoulder between α and the dc and MWS slope.

4.2. Analysis

Based on previous experience, model functions have been fitted to the dielectric data, with Havriliak–Negami (H–N) [36]

$$\varepsilon^*(\omega) = \varepsilon_\infty + \frac{\Delta\varepsilon}{\left(1+(i\omega\tau_{HN})^{1-\alpha}\right)^{\beta}} \quad (1)$$

being the most general form. In this expression, $\varepsilon^* = \varepsilon' - i\varepsilon''$, is the complex dielectric function, $\omega = 2\pi f$, f the field frequency, $\Delta\varepsilon$ the intensity (magnitude, strength) of the dielectric process, $\tau_{HN} = 1/(2\pi f_{HN})$ and f_{HN} the position of the relaxation process on the frequency scale, ε_∞ is $\varepsilon'(f)$ for $f \gg f_{HN}$, α and β are shape parameters, representing the symmetrical and asymmetrical broadening of the peak with respect to the Debye peak, respectively. In case $\beta = 1$, Equation (1) reduces to the symmetric Cole–Cole (C–C) equation [26,36].

Local relaxations are known to be symmetric in shape; therefore the C–C equation was fitted to the dielectric loss (imaginary part of the dielectric function) spectra for the γ relaxation. To the complex spectra in the combined α-α'-MWS-dc conductivity region, the sum of i) an H-N term (corresponding to α) ii) a C–C term corresponding to α' and iii) a linear decrease in the log–log representation of the form

$$\varepsilon'' = A\cdot\omega^s \quad (2)$$

for the combined MWS and dc conductivity effect was fitted.

The peak frequency of the α relaxation was calculated by [37]

$$f_{max} = f_{HN}\left[\sin\left[\frac{(1-\alpha)\pi}{2+2\beta}\right]\Big/\sin\left[\frac{(1-\alpha)\beta\pi}{2+2\beta}\right]\right]^{\frac{1}{1-\alpha}} \quad (3)$$

For relaxations of the C–C type (symmetric), obviously $f_{max} = f_{HN}$.

Due to strong overlapping with α, the isothermal spectra in the region of the β relaxation have not been analyzed according to the previous procedure. The same stands also for the spectra of T1400 where the α relaxation exhibits a strong overlap with both β and γ. However, in the T1400 spectra, the α' region was fitted as a sum of a C–C peak and a slope in the log–log plot. Nevertheless, a few points for β relaxation of PU00 have been included in the Arrhenius plot (see below) and are in good agreement with TSDC.

By the fitting procedure described above, information extracted from each relaxation is quantified in terms of time scale (f_{max}), magnitude ($\Delta\varepsilon$) and shape (α and β). However, due to the strong overlapping of the 4 processes in the high temperature range, and the subsequent inaccuracy in the calculated values, only information on the time scale (and to some extent, see below, on the magnitude) was considered as reliable and will be further evaluated in this paper.

Fig. 10 shows the Arrhenius plot (activation diagram) of the Terathane 1400, the neat Polyurethane matrix and the hybrids. Points for the α relaxation of Terathane were determined by reading out the temperature of the dielectric loss maxima from the isochronal plots and assigning them to the respective frequency. In all the other cases, $f_{max}(T)$ was determined by the fitting procedure

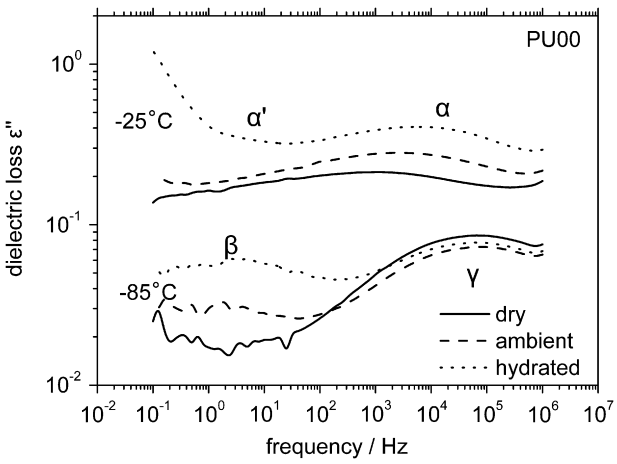

Fig. 9. Comparative dielectric loss spectra of the polyurethane matrix for different hydration levels at two different temperatures.

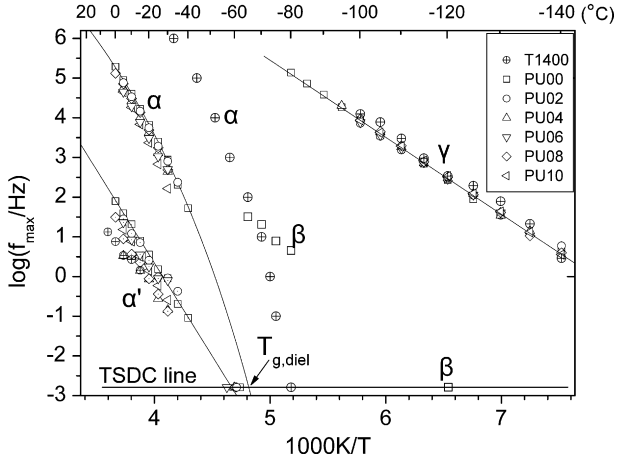

Fig. 10. Arrhenius plot for the γ, α, α' relaxations for all materials under investigation. VTF and Arrhenius curves obtained by fitting for the α and γ relaxations of PU00, respectively, are shown, as well as a straight line as a guide to the eye for the α' relaxation of the same material. A few points for β relaxation of PU00 are also included. TSDC data are included at the equivalent frequency of 1.6×10^{-3} Hz.

described above. In the same plot, TSDC peak temperatures have been included at the equivalent frequency of 1.6×10^{-3} corresponding to a relaxation time of 100 s [25].

It is obvious that the γ relaxation time scale is the same for all materials under investigation, confirming its local character and the fact that it arises from Terathane.

Confirming all previous observations, the α relaxation of the PU is slower by 3 decades in frequency compared to that of pure Terathane, while a further systematic (however not so prominent) decrease of time scale is observed by modification by PHIPOSS.

The data for the temperature dependence of the time scale of the dielectric response were further analyzed by fitting appropriate functions to the $f_{max}(T)$ data for each relaxation. The Arrhenius equation [38]

$$f_{max} = f_0 \cdot \exp\left(-\frac{W}{kT}\right) \quad (4)$$

where W is the activation energy, k Boltzmann's constant and f_0 a frequency factor, was fitted to the data for the secondary γ relaxation and values of $W = 0.39$ eV and $f_0 = 10^{15}$ Hz were obtained for all samples. These values are in the range of values reported for various PUs in previous work [25,34,35].

The Vogel–Tammann–Fulcher (VTF) equation [38]

$$f_{max} = A \cdot \exp\left(-\frac{B}{T - T_0}\right) \quad (5)$$

characteristic of cooperative processes, was fitted to the data for the α relaxation. In this equation A, B and T_0,(Vogel temperature) are temperature independent empirical constants. Following common praxis for reducing the number of fitting parameters, a value of 10^{13} Hz was fixed for the parameter A (preexponential factor) [26,39,40]. Reasonable values were then obtained for B and T_0, the latter being by about 65 °C lower than the calorimetric glass transition temperature (T_g).

Temperatures ($T_{g,diel}$) obtained by extrapolation of the VTF fits to the frequency 1.6×10^{-3} Hz ($\tau = 100$ s), defined as dielectric glass transition temperature [41], were also calculated and plotted in Fig. 3. They are in good agreement with calorimetric T_g and peak temperatures T_a confirming results obtained by DSC and TSDC, respectively.

Values of $\Delta\varepsilon$ for the α relaxation obtained by the fitting procedure described above (Equation (1)) were used to calculate the fraction of immobilized polymer χ_{im} in the hybrids, adopting the same interpretation for the reduction of the dielectric strength in the hybrids and following the same procedure described for TSDC in Section 3.3. First, $\Delta\varepsilon$ was normalized to the same polymer fraction by $\Delta\varepsilon_n = \Delta\varepsilon/(1 - w)$, where w is the weight fraction of POSS in the hybrids, and then χ_{im} was calculated by $\chi_{im} = (\Delta\varepsilon_0 - \Delta\varepsilon_n)/\Delta\varepsilon_0$, where $\Delta\varepsilon_0$ is $\Delta\varepsilon$ in neat PU. The values obtained for χ_{im} are plotted as a function of POSS content in Fig. 5 together with values obtained by TSDC in Section 3.3.

Two additional methods of calculating the relaxation strength $\Delta\varepsilon$ of the $\Delta\varepsilon$ relaxation were also employed. In the first, $\Delta\varepsilon$ at a representative temperature of −25 °C was obtained directly from the corresponding $\varepsilon'(f)$ plots (not shown here) without any fitting procedure as the difference between low- and high-frequency values of ε'. As typically in complex polymeric systems, no well-defined step in $\varepsilon'(f)$ is observed in the frequency range of a loss peak but rather a drop, which limits the accuracy of the method for determining absolute values; trends can be, however, followed well. In the second method, $\Delta\varepsilon$ was obtained from Cole–Cole plots, i.e. from plots of ε'' against ε' with the frequency f as parameter, constructed for the data at −25 °C [42]. $\Delta\varepsilon$ values calculated by these two methods were used to calculate values of χ_{im}, following the procedure described above, which are plotted against POSS content in Fig. 5, together with the DRS data obtained by the fitting analysis and the TSDC data. No DRS data are shown in Fig. 5 for PU06, where the α' relaxation is more pronounced (compare Fig. 8) and calculation of $\Delta\varepsilon'$ is more ambiguous.

Independently of the method of calculation, the results in Fig. 5 suggest, in agreement with each other, that a fraction of polymer in the hybrids is immobilized, i.e. it makes no contribution to the α relaxation (dynamic glass transition). We would like to draw attention to the fact that in the present work and similar work on other polymer nanocomposites [17,21,22,33] the direct experimental result is that of a significant reduction of the response in the nanocomposites. Immobilization of a fraction of the polymer matrix is then a reasonable way to interpret this result. The fraction of immobilized polymer in Fig. 5 increases with increasing POSS content, which is reasonable. A decrease is, however, observed at the highest POSS content of 10%, independently of the method of calculation. This result suggests, in agreement with similar results obtained for other polymer nanocomposites [17,21,22,33], that effects of nanoparticles may become less prominent at higher filler fraction due to decrease of the mean interparticle distance and partial overlapping of regions of the matrix affected. The results in Fig. 5 correlate well with those of thermogravimetric analysis of the same materials indicating a maximum increase in thermal stability at POSS contents ~4–6 wt% [22]. Absolute values of χ_{im} in Fig. 5 show scattering with composition and systematic variation depending on the method of calculation, values obtained by TSDC being systematically larger than corresponding values obtained by DRS. These results are reasonable, bearing in mind limitations in the accuracy of calculations mentioned above. As mentioned in Section 3.3, similar results for the dependence of the fraction of immobilized polymer on filler content were obtained in previous work with poly(dimethyl siloxane)/silica [20], PU/clay [21] and rubbery epoxy networks/POSS [17] nanocomposites. Absolute values of χ_{im} are approximately in the same range of 0–40% for the four nanocomposite systems. In the three systems mentioned above, DSC data were evaluated also with respect to the fraction of immobilized polymer, calculated from the heat capacity jump at the glass transition [20]. This was not done in the present work, bearing in mind larger uncertainties in the determination of χ_{im} from DSC data [33].

The results in Fig. 5, in combination with those in Fig. 3, showing moderate increase of T_g with increasing POSS content in the hybrids, suggest that effects of POSS particles on molecular dynamics of the PU matrix observed in this work are significant with respect to similar effects observed in several other polymer/POSS nanocomposites [14–18]. The main reason for that should be the incorporation of the POSS particles in the structure of the PU matrix by chemical bonding. This is confirmed by a review of the literature on polymer/POSS nanocomposites, as indicated also in papers mentioned in the Introduction [14–18] and shortly discussed there. Unfortunately it is not possible, at least at this stage, to directly compare polymer dynamics in our hybrids with that in nanocomposites prepared by simply mixing the same components. We could also find no papers for comparison in the literature on PU/POSS materials prepared by simply mixing the components. It would be interesting for future work, at least from the fundamental point of view, to prepare and study such a system, or even PU/POSS materials with different binding modes of POSS particles (simply mixed, pendant blocks, network junctions) following similar work in rubbery epoxy/POSS composites [4,17].

4.2.1. The α' relaxation

The α' relaxation has already been observed by Czech et al. [43] in a PU system, using Terathane 2000 (i.e. with $M_w = 2000$) and

MDI as SS and HS, respectively, crosslinked by hyperbranched polyesters. The authors connected this relaxation to the cold crystallization of Terathane 2000 in the PU matrix, observing that both show up in the same temperature region. Although neat T1400 has a considerable degree of crystallinity, as reported in Section 3.2, no sign of crystallinity was observed in the PU matrices under investigation here under the conditions of the DSC experiments reported in Section 3.2, neither during cooling as crystallization peak, nor during heating as cold crystallization or melting, in agreement with the results of WAXD measurements reported in Section 3.1.

Thus, the origin of α' relaxation is not yet clear. In the polyurethanes, it seems to follow the dynamics of α relaxation becoming systematically slower with increasing POSS content. Moreover, it merges with the α relaxation at low frequencies, thus explaining its absence as a standalone peak in TSDC thermograms (Fig. 4). This is the typical behavior of the so-called normal mode relaxation, which is observed in polymers having a dipole moment component along the chain contour and is attributed to fluctuation and orientation of the end-to-end polarization vector of the polymer chain [44,45]. In that case a relaxation with the same behavior in time scale should be observed also in T1400, which is the only component in the PU matrix with a dipole moment component along its chain contour. But this is not the case; instead, a relaxation (already denoted as α') is observed with time scale similar to that observed in PUs (Fig. 10). Projection of the trace of this relaxation to the equivalent frequency of TSDC (1.6×10^{-3} Hz) suggests that a peak should be observed in TSDC thermograms of T1400 in the vicinity of -50 °C. Indeed, a shoulder is present on the low-temperatures side of the MWS peak at about -40 °C (Fig. 4). A possible explanation for that behavior would be the existence of a fraction of T1400 with slower segmental dynamics than that in the bulk. In the case of PUs this fraction is in the vicinity of the hard domains (HS), while in pure T1400 it is located near the crystals in the semicrystalline sample. This explanation is consistent with the results of several studies in semicrystalline polymers showing the existence of a second slower segmental relaxation (often denoted as α_c [34]), related with the motion of amorphous regions constrained by the crystalline phase [46].

Experimental evidence for the relationship between the α' relaxation and crystallinity in the case of T1400 is shown in Fig. 11. For the experiments shown there the sample was melted at 30 °C, cooled to 18 °C, which was then fixed, and isothermal crystallization was followed by DRS. The temperature of 18 °C was chosen on the basis of preliminary DSC isothermal crystallization experiments as a suitable temperature to complete crystallization within a few h. 20 spectra in the typical 10^{-1}–10^{6} Hz range starting from high frequencies, were recorded consecutively, each run lasting ~7 min, thus making a ~2.5 h total duration of the experiment. The first run shows only dc conductivity contribution (a linear increase of loss with decreasing frequency with slope -1 in the log–log plot; deviation in the low frequency region is explained by the ongoing crystallization process). While crystallization proceeds (as indicated by the DSC experiments not shown here), conductivity contribution is reduced and a relaxation emerges. After 8 runs (~1 h) the spectrum remains unchanged clearly revealing the α' relaxation and, thus, connecting that relaxation with crystallinity in neat T1400.

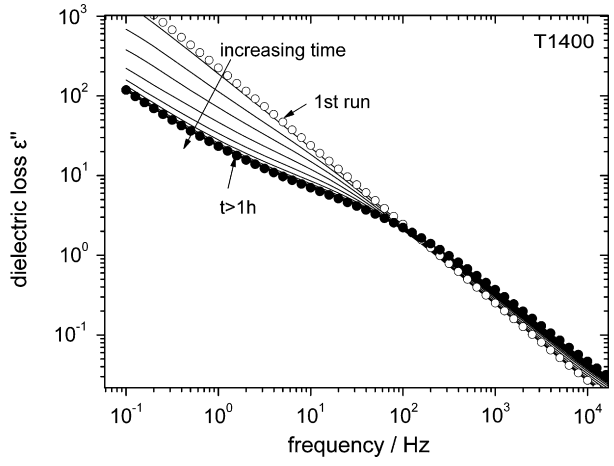

Fig. 11. Repetitive dielectric loss spectra of T1400 at 18 °C during crystallization. Each run lasts 7 min and starts from high frequencies. First and last run are stressed by plotting as open and filled circles, respectively.

5. Conclusions

Results reported in the literature on effects of nanoparticles on polymer dynamics in polymer nanocomposites, in particular on segmental dynamics and glass transition, are often controversial. We think that, for a proper investigation, morphology, in particular quality of particle dispersion, should be carefully controlled [20]. In addition, polymer–filler interactions and effects on molecular packing of the chains should be properly considered [17]. Results on glass transition and segmental dynamics in PU/POSS hybrids by DSC, TSDC and DRS in the present work show, in good agreement with each other, slight increase of the PU glass transition temperature by maximum 5 °C upon modification by POSS, indicating slower dynamics in the hybrids. At the same time the magnitude of the α relaxation (dynamic glass transition) by both TSDC and DRS decreases significantly in the hybrids. Following similar work on other polymer nanocomposites, this last result is interpreted in terms of a fraction of polymer being immobilized, i.e. making no contribution to the α relaxation. Thus, effects of POSS particles on polymer dynamics in the PU/POSS hybrids under investigation are rather strong compared to similar systems reported in the literature. We think that the method of preparation of the hybrids with the POSS particles being tethered on the chains is the main reason for that. It would be interesting to include in the investigation in future work various PU/POSS materials with different binding modes of the POSS particles.

In addition to polymer–filler interactions, the quality of dispersion of nanoparticles in the polymer matrix may significantly affect polymer dynamics [20,47]. The results of AFM measurements indicate the formation of POSS crystallites in the PU/POSS hybrids under investigation here, in particular extended structures at low POSS content and more regular, smaller structures at higher POSS content. These results correlate well with those of the combined DSC/TSDC/DRS studies showing moderate increase of glass transition temperature with increasing POSS content at low filler contents, followed by a steeper increase at higher filler contents (Fig. 3). Obviously, the smaller POSS structures are more effective in slowing down segmental dynamics due to the resulting higher surface-to-volume ratio. On the other hand, the fraction of immobilized polymer decreases at the highest POSS content of 10% (Fig. 5), obviously due to decrease of the mean interparticle distance with increasing POSS content resulting in overlapping of the regions (layers) of immobilized polymer. The results in Fig. 5 correlate well with those of thermogravimetric analysis of the same hybrids indicating a maximum increase in thermal stability at POSS contents ~4–6 wt% [22]. Results on polymer dynamics, similar to those reported here, provide a basis for modeling in future work various properties of the hybrids, such as mechanical properties and thermal stability.

A peculiarity of the PU/POSS hybrids under investigation here is that the polymer matrix is a microphase-separated one. The properties of the neat PU matrix depend sensitively on the degree of microphase separation. Thus, in addition to any direct reinforcing effects of the filler, glass transition and segmental dynamics, as well as the final technological properties of the hybrids, could be also indirectly affected by a modification of the degree of microphase separation by the filler. The TSDC results for the MWS interfacial polarization/relaxation (Fig. 4) provide convincing evidence that this is not the case here. Work is in progress on other PU/POSS nanocomposites with a different composition of the PU matrix to further follow this point. It is interesting to note in this connection that in the case of a microphase-separated polymer matrix the nanoparticles may be preferably assembled in one of the two phases, giving rise to interesting morphologies and properties [48]. This provides an additional motivation for investigating in future work PU/POSS nanocomposites prepared by simply mixing the two components. The work in progress on PU/POSS nanocomposites with a variation of the composition of the PU matrix mentioned above will be of interest also with respect to the origin of the α' relaxation in PUs, as it may provide a possibility to further check the hypothesis put forward in this work that this relaxation is the slower segmental relaxation of regions of the soft microphase located in the vicinity of and constrained by the hard microdomains.

Acknowledgements

This work has been partially supported by the Polish Ministry of Science and Higher Education under contract No. N N507 3657 33.

K.R. acknowledges financial support by the NTUA.

Appendix. Supplementary material

Fig. S1.

Fig. S2.

Note: Supplementary material associated with this article can be found in the online version, at doi:10.1016/j.polymer.2009.11.067.

References

[1] Gleiter H. Acta Mater 2000;48:1–29.
[2] Kickelbick G. Prog Polym Sci 2003;28:83–144.
[3] Sanchez C, Soller Illia GJ de AA, Ribot F, Lalot T, Mayer CR, Cabuil V. Chem Mater 2001;13:3061–83.
[4] Matejka L, Strachota A, Plestil J, Whelam P, Steinhardt M, Slouf M. Macromolecules 2004;37(25):9449–56.
[5] Pielichowski K, Njuguna J, Janowski B, Pielichowski J. Adv Polym Sci 2006;201:225–96.
[6] Bliznyuk VN, Tereshchenko TA, Gumenna MA, Gomza YuP, Shevchuk AV, Klimenko NS, et al. Polymer 2008;49:2298–305.
[7] Charnetskaya AG, Polizos G, Shtompe VI, Privalko EG, Kercha YuYu, Pissis P. Eur Polym J 2003;39:2167–74.
[8] Georgoussis G, Kanapitsas A, Pissis P, Savelyev YuV, Veselov VYa, Privalko EG. Eur Polym J 1999;36:1113–26.
[9] Koberstein JT, Galambos AF, Leung LM. Macromolecules 1992;25:6195–204.
[10] Liu H, Zheng S. Macromol Rapid Commun 2005;26:196–200.
[11] Fu BX, Gelfer MY, Hsiao BS, Phillips S, Viers B, Blanski R, et al. Polymer 2003;44:1499–506.
[12] Lichtenhan JD, Haddad TS, Schwab JJ, Carr MJ, Chaffe KP, Mather PT. Polym Preprints 1998;39:489–90.
[13] Fu BX, Hsiao BS, Pagola S, Stephens P, White H, Rafailovich M, et al. Polymer 2001;42:599–611.
[14] Zhao Y, Schiraldi DA. Polymer 2005;46(25):11640–7.
[15] Xu HY, Kuo SW, Lee JS, Chang FC. Macromolecules 2002;35(23):8788–93.
[16] Kopesky ET, Haddad TS, Cohen RE, McKinley GH. Macromolecules 2004;37(24):8992–9004.
[17] Kourkoutsaki Th, Logakis E, Kroutilova I, Matejka L, Nedbal J, Pissis P. J Appl Polym Sci 2009;113(4):2569–82.
[18] Hao N, Boehning M, Goering H, Schoenhals A. Macromolecules 2007;40(8):2953–64.
[19] Kim EH, Myoung SW, Jung YG, Paik U. Prog Org Coat 2009;64:205–9.
[20] Fragiadakis D, Pissis P. J Non-Cryst Solids 1997;353:4344–52.
[21] Kripotou S, Pissis P, Savelyev YV, Robota LP, Travinskaya TV. J Macromol Sci B, in press.
[22] Janowski B, Pielichowski K. Thermochim Acta 2008;478:51–3.
[23] Raftopoulos K, Pandis Ch, Apekis L, Pissis P, Pielichowski K, Janowski B. Mod Polym Mater Env Appl 2008;3:209–14.
[24] van Turnhout J. Thermally stimulated discharge of electrets. In: Sessler GM, editor. Electrets, topics in applied physics, vol. 33. Berlin: Springer; 1980. p. 81–215.
[25] Kanapitsas A, Pissis P. Eur Polym J 2000;36:1241–50.
[26] Kremer F, Schoenhals A, editors. Broadband dielectric spectroscopy. Berlin Heidelberg: Springer Verlag; 2003.
[27] Bershtein VA, Egorova LM, Yakushev PN, Pissis P, Sysel P, Brozova L. J Polym Sci Pol Phys 2002;40:1056–69.
[28] Apekis L, Pissis P, Christodoulides C, Spathis G, Niaounakis E, Kontou E, et al. Prog Coll Polym Sci 1992;90:144.
[29] Vatalis AS, Delides CG, Georgoussis G, Kyritsis A, Grigorieva OP, Sergeeva LM, et al. Thermochim Acta 2001;371:87–93.
[30] Tsonos C, Apekis L, Zois C, Tsonos G. Acta Mater 2004;52:1319–26.
[31] Hamon BV. Aust J Phys 1953;6(3):304–14.
[32] Kotsilkova R, Fragiadakis D, Pissis P. J Polym Sci Pol Phys 2005;43:522–33.
[33] Sargsyan A, Tonoyan A, Davtyan S, Schick C. Eur Polym J 2007;43:3113–27.
[34] Kanapitsas A, Lebedev E, Slisenko O, Grigoryeva O, Pissis P. J Appl Polym Sci 2006;101:1021.
[35] Pissis P, Apekis L, Christodoulides C, Niaounakis M, Kyritsis A, Nedbal J. J Polym Sci Pol Phys 2006;34:1529–39.
[36] Havriliak Jr S, Havriliak SJ. Dielectric and mechanical relaxation in materials: analysis, interpretation, and application to polymers. Munich: Hanser; 1997.
[37] Diaz-Calleja R. Macromolecules 2000;33(24):8924.
[38] Donth E. The glass transition: relaxation dynamics in liquids and disordered materials. Berlin Heidelberg: Springer Verlag; 2001.
[39] Kripotou S, Pissis P, Kontou E, Fainleib AM, Grigoryeva O, Bey I. Polym Bull 2007;58:93–104.
[40] Richert R, Angell CA. J Chem Phys 1998;108(21):9016–26.
[41] Barut G, Pissis P, Pelster R, Nimtz G. Phys Rev Lett 1998;80(16):3543–6.
[42] Espadero Berzosa A, Gomez Ribelles JL. Macromolecules 2004;37:6472–9.
[43] Czech P, Okrasa L, Mechin F, Boiteux G, Ulanski J. Polymer 2006;47:7207–15.
[44] Kosma S, Raftopoulos K, Pissis P, Strachota A, Matejka L, Ribot F, et al. J Nanostruct Polym Nanocomposites 2007;3(4):144–56.
[45] Watanabe H, Yamada H, Urakawa O. Macromolecules 1995;28:6443–53.
[46] Napolitano S, Wuebbenhorst M. Macromolecules 2007;353:4357–61.
[47] Robertson CG, Lin CJ, Rackaitis M, Roland CM. Macromolecules 2008;41:2727–31.
[48] Balazs AC. Curr Opin Solid State Mater Sci 2003;7:27–33.